Report

Current Biology

Suppression of Plant Immunity by Fungal Chitinase-like Effectors

Graphical Abstract

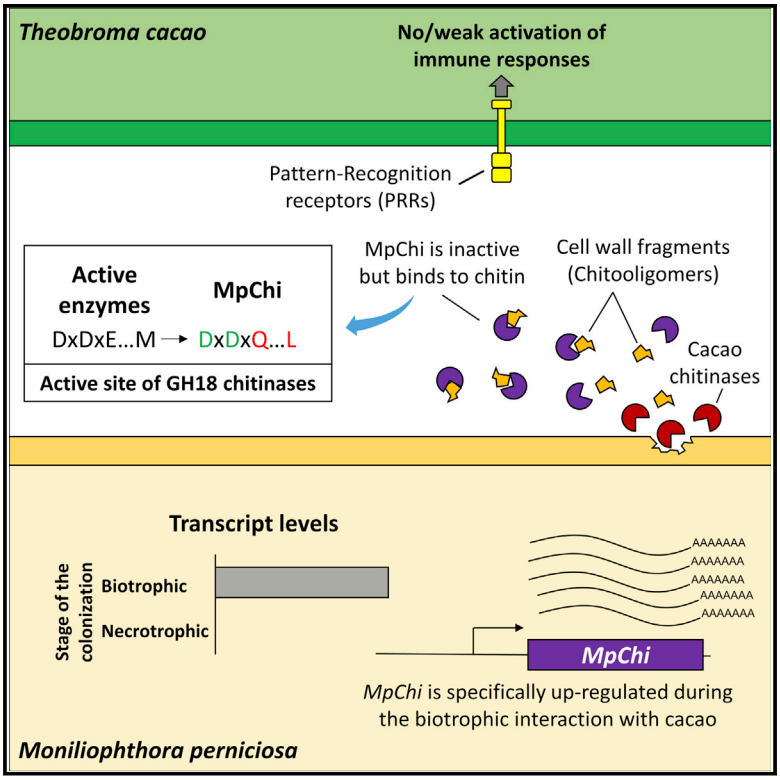

Highlights

- Two fungal pathogens of cacao express inactive chitinases during the infection
- Despite being catalytically dead, these proteins retain the ability to bind chitin
- Inactive chitinases prevent plant immunity by sequestering free chitin fragments
- Neofunctionalization of enzymes is a pathway for the evolution of fungal effectors

Authors

Gabriel Lorencini Fiorin, Andrea Sanchéz-Vallet, Daniela Paula de Toledo Thomazella, ..., Bart P.H.J. Thomma, Gonçalo Amarante Guimarães Pereira, Paulo José Pereira Lima Teixeira

Correspondence

goncalo@unicamp.br (G.A.G.P.), paulojt@email.unc.edu (P.J.P.L.T.)

In Brief

Fiorin et al. demonstrate that two fungal pathogens of cacao independently evolved catalytically dead chitinases that bind to chitin and prevent elicitation of plant immunity. The study exemplifies how pathogens may evolve effectors by repurposing the functions of enzymes that are conserved throughout evolution.

Fiorin et al., 2018, Current Biology *28*, 3023–3030
September 24, 2018
https://doi.org/10.1016/j.cub.2018.07.055

CellPress

Current Biology
Report

Suppression of Plant Immunity by Fungal Chitinase-like Effectors

Gabriel Lorencini Fiorin,[1,2] Andrea Sanchéz-Vallet,[3,4] Daniela Paula de Toledo Thomazella,[5] Paula Favoretti Vital do Prado,[1,2] Leandro Costa do Nascimento,[2,6] Antonio Vargas de Oliveira Figueira,[7] Bart P.H.J. Thomma,[3] Gonçalo Amarante Guimarães Pereira,[2,*] and Paulo José Pereira Lima Teixeira[8,9,*]
[1]Graduate Program in Genetics and Molecular Biology, Instituto de Biologia, Universidade de Estadual de Campinas, Campinas 13083-970, Brazil
[2]Laboratório de Genômica e Expressão, Departamento de Genética, Evolução e Bioagentes, Instituto de Biologia, Universidade Estadual de Campinas, Campinas 13083-970, Brazil
[3]Laboratory of Phytopathology, Wageningen University and Research, Droevendaalsesteeg 1, 6708 Wageningen, the Netherlands
[4]Plant Pathology, Institute of Integrative Biology, ETH Zurich, 8092 Zurich, Switzerland
[5]Department of Plant and Microbial Biology, University of California, Berkeley, Berkeley, CA 94720, USA
[6]Centro Nacional de Processamento de Alto Desempenho, Universidade Estadual de Campinas, Campinas 13083-970, Brazil
[7]Laboratório de Melhoramento de Plantas, Centro de Energia Nuclear na Agricultura, Universidade de São Paulo, Campus "Luiz de Queiroz," Piracicaba 13400-970, Brazil
[8]Department of Biology, University of North Carolina at Chapel Hill, Chapel Hill, NC 27599, USA
[9]Lead Contact
*Correspondence: goncalo@unicamp.br (G.A.G.P.), paulojt@email.unc.edu (P.J.P.L.T.)
https://doi.org/10.1016/j.cub.2018.07.055

SUMMARY

Crop diseases caused by fungi constitute one of the most important problems in agriculture, posing a serious threat to food security [1]. To establish infection, phytopathogens interfere with plant immune responses [2, 3]. However, strategies to promote virulence employed by fungal pathogens, especially non-model organisms, remain elusive [4], mainly because fungi are more complex and difficult to study when compared to the better-characterized bacterial pathogens. Equally incomplete is our understanding of the birth of microbial virulence effectors. Here, we show that the cacao pathogen *Moniliophthora perniciosa* evolved an enzymatically inactive chitinase (MpChi) that functions as a putative pathogenicity factor. *MpChi* is among the most highly expressed fungal genes during the biotrophic interaction with cacao and encodes a chitinase with mutations that abolish its enzymatic activity. Despite the lack of chitinolytic activity, MpChi retains substrate binding specificity and prevents chitin-triggered immunity by sequestering immunogenic chitin fragments. Remarkably, its sister species *M. roreri* encodes a second non-orthologous catalytically impaired chitinase with equivalent function. Thus, a class of conserved enzymes independently evolved as putative virulence factors in these fungi. In addition to unveiling a strategy of host immune suppression by fungal pathogens, our results demonstrate that the neofunctionalization of enzymes may be an evolutionary pathway for the rise of new virulence factors in fungi. We anticipate that analogous strategies are likely employed by other pathogens.

RESULTS AND DISCUSSION

Plants possess an innate immune system that recognizes and responds to potential invaders [2]. Extracellular surveillance of non-self molecules is mediated by cell surface receptors that are activated upon recognition of microbial-associated molecular patterns (MAMPs). These are often highly conserved molecules with indispensable functions in whole classes of microbes (e.g., chitin, β-glucans, and flagellin). Activation of such receptors signals to an immune response known as MAMP-triggered immunity (MTI), which involves the production of reactive oxygen species, ion fluxes, and transcriptional reprogramming and synthesis of an array of new proteins whose combined action halts pathogen growth [2]. Pathogens, on the other hand, have evolved sophisticated strategies mediated by effector molecules to prevent or interfere with MTI and thus promote infection [3].

Chitin is a polymer of N-acetylglucosamine (NAG) and a structural component of the cell wall in fungi. Chitin fragments are potent MAMPs and elicit MTI in many species of plants [5–8]. Suppression of chitin-triggered immunity is emerging as a major aspect of fungal virulence [9]. To prevent chitin-triggered immunity, some ascomycete pathogens utilize effectors containing the carbohydrate-binding LysM (lysin motif) domain to sequester cell-wall fragments that would otherwise be perceived by plant receptors [10–14]. Given the strong selection pressure imposed by the arms race with the plant immune system, strategies to mitigate chitin-triggered immunity are likely to have evolved multiple independent times in fungal pathogens [9]. However, the diversity of mechanisms used by fungi to achieve this suppression is essentially unknown.

Theobroma cacao is a tropical tree native to the Amazon whose beans are the source of chocolate. Currently, the

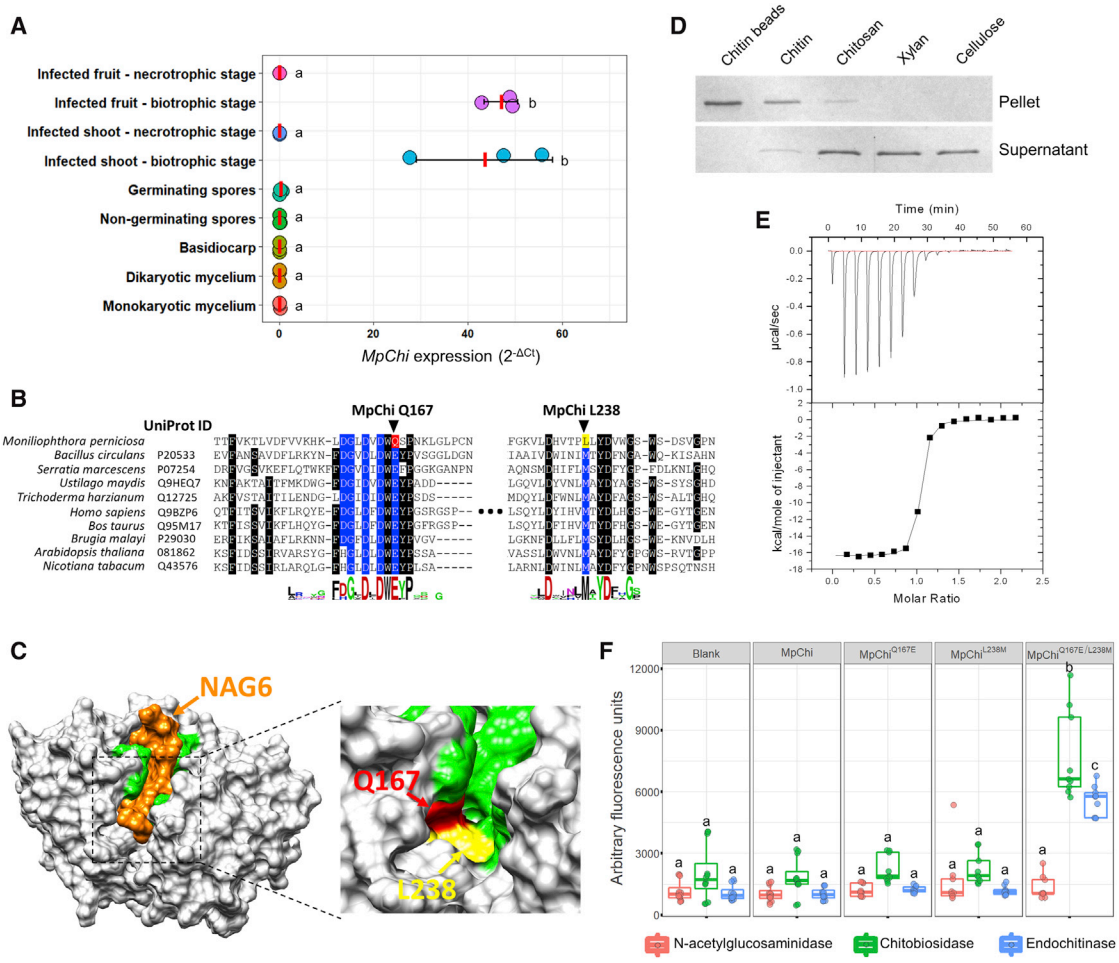

Figure 1. The *M. perniciosa MpChi* Gene Encodes a Chitinase-like Protein that Binds to Chitin but Lacks Enzymatic Activity due to at Least Two Mutations in Its Catalytic Site

(A) *MpChi* is highly expressed during the biotrophic stage of WBD. Data were acquired by qPCR and were normalized using the *M. perniciosa* β-*actin* and *IF3b* genes. Red bars and whiskers represent the mean and the SD from three biological replicates, respectively. Letters represent conditions with significant differences according to the post hoc ANOVA Tukey's test ($p < 0.05$). The *MpChi* expression profile in 41 RNA-seq libraries is shown in Figure S1A.

(B) MpChi has substitutions in residues that are highly conserved in GH18 chitinases (E167Q and M238L; labeled in red and yellow, respectively). See also Figure S1B.

(C) Homology modeling of the MpChi structure revealed that the two substituted residues (Q167, red; L238, yellow) form an interface in the catalytic pocket. Aromatic amino acids involved in chitin binding are conserved (green).

(D) Pull-down assay demonstrates that MpChi binds to chitin, but not to chitosan, xylan, or cellulose. The degree of deacetylation of the chitosan preparation used in the experiment was 85%; thus, the weak band observed in the pellet fraction is likely due to the presence of residual chitin in the reagent (i.e., acetylated chitosan).

(E) Isothermal titration calorimetry (ITC) shows that MpChi binds to chitohexaose (NAG6) with high affinity (Kd = 13 nM) and 1:1 stoichiometry.

(F) MpChi lacks enzymatic activity, which can be rescued by reverting the two mutated residues to the consensus amino acids of GH18 enzymes. See also Figure S1C. At least nine measurements were taken per condition in three independent experiments. Letters represent conditions with significant differences according to the post hoc ANOVA Tukey's test ($p < 0.05$). Circular dichroism showed that the recombinant proteins used in these experiments were properly folded (see Figure S2A).

livelihoods of over 40 million people depend on this crop, which is affected by devastating diseases that threaten the supply and quality of cocoa beans produced worldwide. Three major pathogens cause an estimated annual loss of 20%–40% in the global production of cocoa beans [15], namely the basidiomycetes *Moniliophthora perniciosa* (causing witches' broom disease [WBD]) and *M. roreri* (causing frosty pod rot [FPR]) and oomycetes of the genus *Phytophthora* (causing black pod rot [BPR]). Although BPR is present worldwide, WBD and FPR remain restricted to the Americas and constitute a major bottleneck for cacao production on this continent [16]. Because there are no effective control measures to these diseases, their spread to other continents could have a severe impact on the chocolate industry, with a catastrophic socioeconomic outcome.

To gain insights into the WBD biology, we recently constructed a comprehensive transcriptome atlas for *M. perniciosa* and cacao [17]. The fungus *M. perniciosa* is a hemibiotrophic pathogen

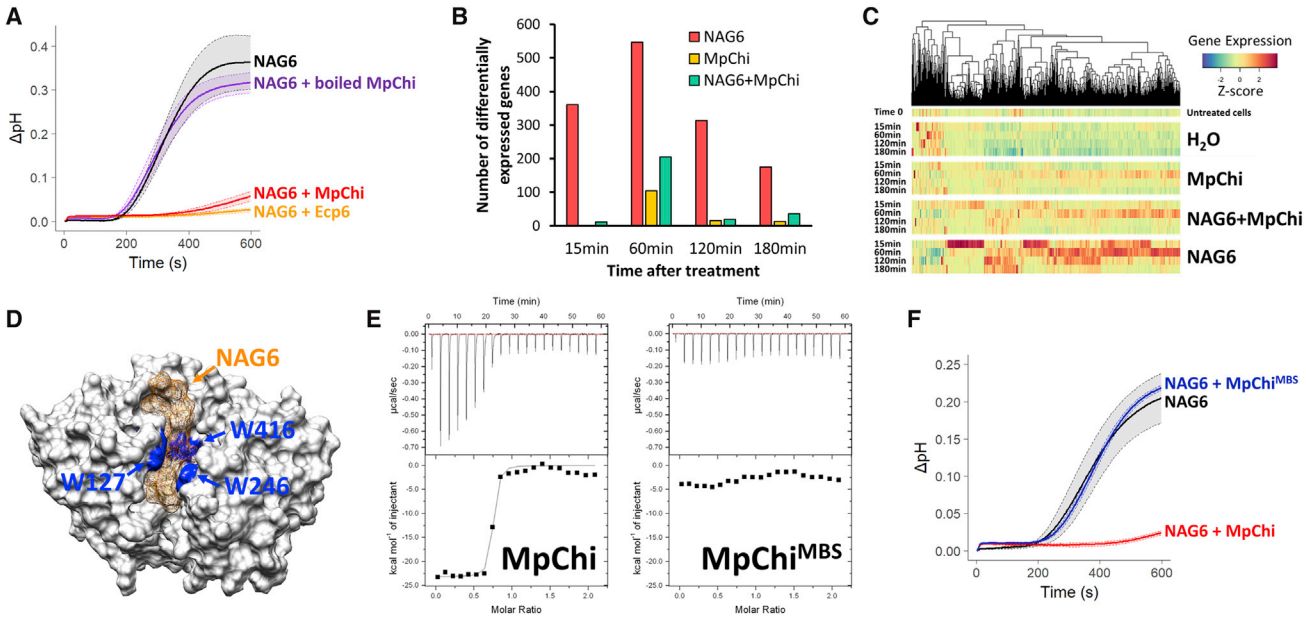

Figure 2. MpChi Binds to Free Chitin Oligomers and Prevents MTI

(A) Medium alkalinization induced by the treatment of tobacco cells with 10 nM chitin oligomers (NAG6) is prevented by MpChi. The graph shows the pH shift of the medium over 10 min after treatment with NAG6. Heat-treated MpChi (96°C for 5 min) and the *Cladosporium fulvum* LysM effector Ecp6 were used as negative and positive controls, respectively. Shades show the SD of three biological replicates. See also Figure S3.

(B) Number of genes differentially expressed over time (15, 60, 120, and 180 min) in tobacco cells treated with 10 nM NAG6, MpChi, or NAG6+MpChi. Data were acquired by RNA-seq.

(C) Heatmap of the *Z* score transformed expression values of genes that responded to at least one of the treatments in the RNA-seq experiment. MpChi mitigates the activation of NAG6-responsive genes.

(D–F) MpChi^{MBS} contains alanine substitutions in three tryptophans (D; blue in the homology model) involved in substrate binding (see also Figure S1B), (E) has impaired capacity to bind to NAG6, and (F) is unable to prevent NAG6-triggered medium alkalinization in tobacco cells. Shades show the SD of three biological replicates. Circular dichroism showed that the recombinant proteins used in these experiments were properly folded (see Figure S2A).

that colonizes the living tissues of the host plant for one to three months before switching to a destructive necrotrophic stage that kills and feeds off host dead tissue [18]. The analysis of dual RNA sequencing (RNA-seq) libraries of the WBD progression revealed fungal genes that are specifically expressed in the biotrophic stage of the disease. This set of genes is highly enriched in candidate virulence factors [17]. Curiously, a gene encoding a putative chitinase of the glycoside hydrolase family 18 (GH18) is distinctively expressed during the biotrophic interaction with cacao (Figures 1A and S1A). This gene, named *MpChi*, is among the most highly expressed fungal genes in infected cacao tissues (Table S1), suggesting a role in pathogenicity.

Chitinases belonging to the family GH18 are present in all domains of life with functions that include development, parasitism, nutrition, and immunity [19, 20]. Remarkably, the glutamate (E) that comprises the catalytic motif of GH18 chitinases (DxxDxDxE) is replaced by a glutamine (Q167) in MpChi (Figure 1B). This glutamate is highly conserved in GH18 chitinases and donates a proton that is required for substrate hydrolysis [21]. Furthermore, a closer inspection of the MpChi amino acid sequence revealed a second substitution in another conserved residue (L238; Figure 1B). Although these two residues (Q167 and L238) are 70 amino acids apart in the protein sequence, they localize next to each other in the modeled tertiary structure (Figure 1C), forming an interface in the catalytic pocket where the cleavage of the substrate occurs.

Despite the substitutions in the catalytic site, aromatic residues required for binding and stabilization of the substrate [21–24] are conserved in MpChi (Figures 1C and S1B). This suggests that this protein lacks chitinolytic activity but retains the ability to bind chitin. Pull-down assays using recombinant MpChi confirmed that it binds efficiently to chitin, but not to chitosan, xylan, or cellulose (Figure 1D). Moreover, isothermal titration calorimetry (ITC) demonstrated that MpChi binds chitin oligomers (NAG6) with high affinity (Kd = 13 nM; Figure 1E). In agreement with the mutations identified in the catalytic site, no chitinolytic activity was detected for MpChi (Figure 1F). However, a version of this protein in which both the glutamine at position 167 and the leucine at position 238 were reverted to the residues that are highly conserved in GH18 chitinases (i.e., glutamate and methionine, respectively) had enzymatic activity. Reversion of each of these residues individually did not result in measurable chitinolytic activity (Figures 1F, S1C, and S2A). Hence, MpChi has no enzymatic activity due to substitutions of at least two highly conserved amino acids in the catalytic pocket of GH18s.

During infection, plants secrete an array of hydrolytic enzymes to impair the development of the invader organism [25]. We thus hypothesized that MpChi would bind to chitin molecules in the fungal cell wall to shield it against lytic plant enzymes. Such strategy was first described for the fungal effector Avr4 from the tomato pathogen *Cladosporium fulvum* [26]. Unlike Avr4, MpChi is unable to shield *Trichoderma viride* cells against lytic enzymes

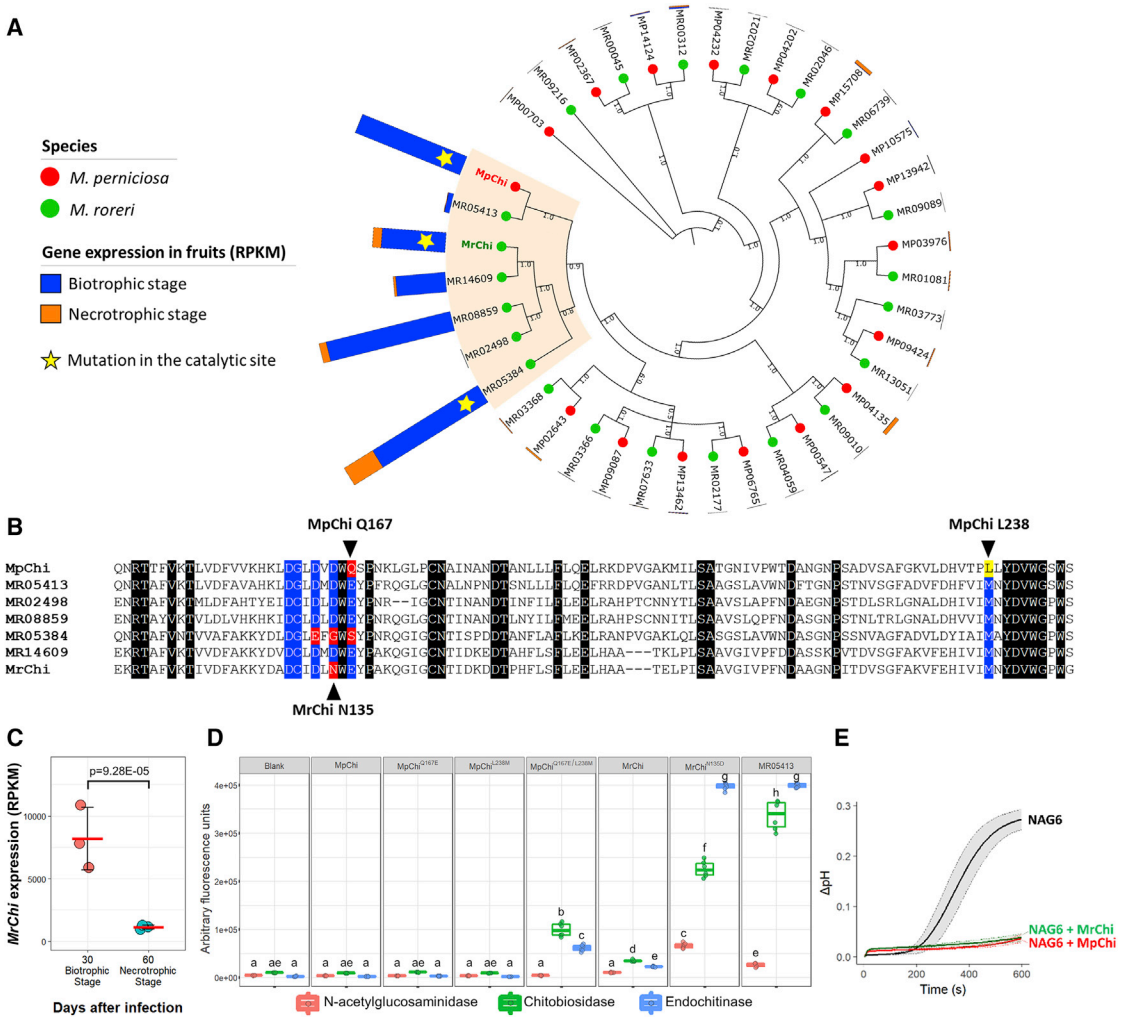

Figure 3. *Moniliophthora roreri* Encodes Additional Chitinase-like Effectors with Independent Substitutions in the Catalytic Site

(A) MpChi and MrChi (labeled in red and green, respectively) are not orthologs and are part of a clade of GH18-encoded genes that are highly expressed during the biotrophic interaction with cacao (gene expression shown as bars). The *M. roreri* protein MR05384 also has a degenerated catalytic site. The cladogram was constructed based on Bayesian inference using the GH18 domains of 17 *M. perniciosa* and 22 *M. roreri* proteins (isolates CP02 and MCA2977, respectively). See also Figure S4A.

(B) Amino acid alignment of proteins belonging to the MpChi/MrChi clade (colored in the cladogram). MpChi, MrChi, and MR05384 have specific substitutions in the catalytic motifs.

(C) *MrChi* is highly expressed during the biotrophic interaction of *M. roreri* with cacao (n = 3).

(D) The MrChi mutation reduces its chitinolytic activity. The variant MrChi^{N135D}, in which the asparagine was reverted to the conserved aspartate, presents higher chitinolytic activity. At least six measurements were taken per condition in two independent experiments. Letters represent conditions with significant differences according to the post hoc ANOVA Tukey's test ($p < 0.05$).

(E) Medium alkalinization induced by the treatment of tobacco cells with 10 nM chitin oligomers (NAG6) is inhibited by MrChi. The graphic shows the pH shift of the medium over 10 min after treatment with NAG6. Shades show the SD of three biological replicates. Chitin-binding assays for MrChi are shown in Figures S2B and S2C.

(Figure S3A). Although we have not tested whether MpChi binds to the *M. perniciosa* biotrophic hyphae during cacao infection, effectors so far proposed to shield fungal hyphae against hydrolysis by plant enzymes were able to protect *T. viride* in the same assay and at much lower concentrations [11, 12, 26]. Therefore, MpChi is unlikely to function in the protection of fungal cell wall against plant hydrolytic enzymes. We next tested whether MpChi is able to prevent the elicitation of chitin-triggered immunity in plants by sequestering free chitin oligomers. Treatment of plant cells with the chitin oligomer NAG6 results in rapid medium alkalinization as a consequence of the ion fluxes across the plasma membrane during MTI [5, 27]. Remarkably, NAG6-induced medium alkalinization was strongly suppressed by MpChi in tobacco cells (Figure 2A). Interference with MTI was also demonstrated by the ability of MpChi to prevent activation of NAG6-induced genes (Figures 2B and 2C). Importantly, a version of MpChi in which we performed alanine substitutions of three tryptophans that are involved in substrate binding

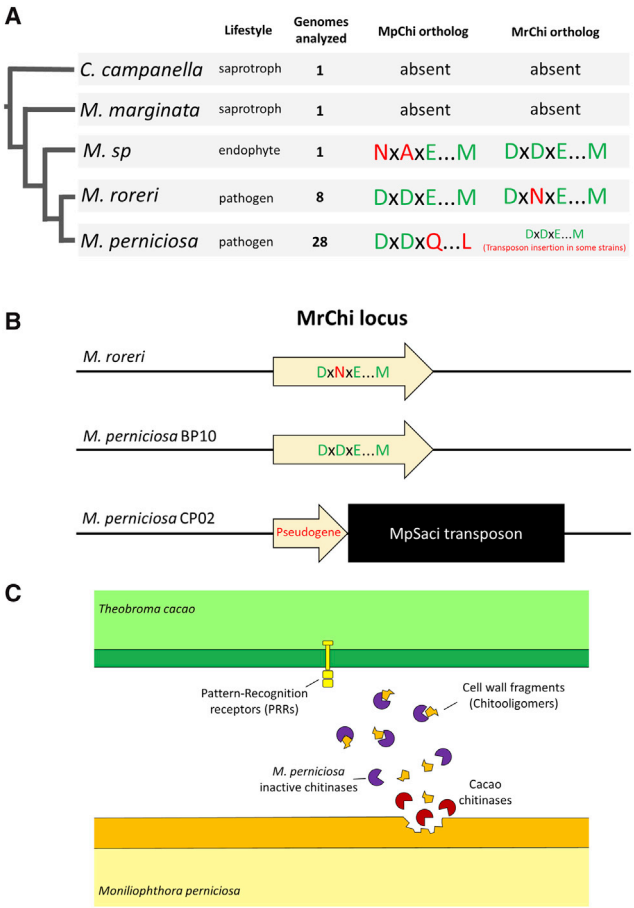

Figure 4. Chitinase-like Effectors Are Present in Multiple Genomes of Pathogenic *Moniliophthora* Species

(A) Summary of the search for chitinase-like effectors in 38 *Moniliophthora* genomes and in *Crinipellis campanella*. *MpChi* alleles encoding proteins with substitutions in the catalytic site were found in all 28 *M. perniciosa* genomes and also in an unnamed grass endophyte from North America. The *MrChi* gene, which is mutated in *M. roreri*, was either found without mutations or interrupted by a transposon insertion in *M. perniciosa*. The saprotrophic species *M. marginata* and *C. campanella* do not contain mutated GH18s in their genomes.

(B) Representation of the *MrChi* locus in *M. roreri* and *M. perniciosa*. BP10 and CP02 are representative isolates encoding intact and truncated genes in *M. perniciosa*, respectively.

(C) Cartoon model illustrating the proposed role for the inactivated chitinases of the *Moniliophthora* pathogens. During infection, fungal cell wall fragments are released due to the action of plant lytic enzymes or as a consequence of fungal growth. These fragments can be perceived by plant receptors and act as MAMPs. *Moniliophthora* pathogens evolved inactivated chitinases that bind to and sequester free chitin fragments to prevent MTI. Fungal LysM proteins are not distinctively expressed during the biotrophic interaction between *M. perniciosa* and cacao (see Figure S4B).

(Figures 2D, 2E, and S1B) was unable to prevent medium alkalinization upon NAG6 treatment (Figure 2F), demonstrating that MpChi requires substrate binding capacity to interfere with MTI. Moreover, MpChi was unable to prevent medium alkalinization triggered by the flagellin epitope flg22, a bacterial elicitor, further demonstrating that MpChi functions through the specific sequestration of chitin fragments (Figure S3B).

We identified 17 GH18-encoding genes in the *M. perniciosa* genome (isolate CP02), with MpChi being the only one with substitutions in the catalytic glutamate (Figure S4A). We next searched for GH18-encoding genes in *M. roreri* [28], a sister species that causes FPR in cacao. Remarkably, the MpChi ortholog in *M. roreri* (MR05413) has canonical residues in its catalytic site and is enzymatically active (Figures 3A, 3B, and 3D). However, a paralog gene in *M. roreri* (*MrChi*), which is highly expressed during the biotrophic interaction of *M. roreri* and cacao (Figure 3C), encodes a GH18 with an independent substitution in one of the aspartates of the catalytic motif (D135N; Figure 3B). This substitution results in reduced enzymatic activity (Figure 3D). Like MpChi, MrChi binds to chitin and prevents chitin-triggered immunity in tobacco cells (Figures 3E, S2B, and S2C). Notably, these proteins belong to a clade in which orthology is less well defined in comparison to the rest of the GH18 family (Figure 3A), indicating the occurrence of multiple gains and/or losses events during the evolution of these pathogens. Moreover, five of the seven genes in this clade are highly expressed during the biotrophic stage of the interaction with cacao, suggesting that at least part of them function as virulence factors. Remarkably, MR05384 in *M. roreri* (Figures 3A and 3B) also contains a degenerated catalytic site and is, therefore, likely enzymatically inactive. Thus, mutated GH18s have evolved independently in these pathogens, consistent with their role as virulence effectors.

We also searched for *MpChi* and *MrChi* alleles in the genomes of 28 *M. perniciosa* and 8 *M. roreri* isolates from diverse geographic locations throughout Latin America. Importantly, the two substitutions in the MpChi catalytic site (E167Q and M238L) were found in all *M. perniciosa* isolates, whereas no substitutions were detected in the different *M. roreri* genomes (Figure 4A). Furthermore, although *MrChi* alleles containing the consensus catalytic residues were found in *M. perniciosa*, some isolates contained an insertion of an MpSaci transposon (Figures 4A and 4B) that likely inactivates this gene [29]. Interestingly, the *MpChi* ortholog of an unnamed *Moniliophthora* species (*M. sp*), isolated as a grass endophyte in North America [30], also encodes a protein with substitutions in the catalytic site, but these substitutions are different from the ones found in *M. perniciosa* (Figure 4A). Remarkably, the saprotrophic species *M. marginata* (isolated from wood debris in Malaysia) [31] and *Crinipellis campanella* (a representative of the closely related *Crinipellis* genus) do not contain GH18s with substitutions in the catalytic site, indicating that the loss of enzymatic activity of chitinases in *Moniliophthora* is associated with a pathogenic and/or endophytic lifestyle.

Thus, two cacao pathogens of the genus *Moniliophthora* have independently evolved inactive chitinases that retain substrate binding ability and are able to prevent chitin-triggered immunity in plants by sequestering free chitin fragments (Figure 4C). These proteins are mechanistically analogous to LysM effectors, exemplify the plasticity of phytopathogens in developing virulence strategies, and underscore the importance of suppression of chitin-triggered immunity for host invasion. Interestingly, none of the seven genes encoding LysM proteins in *M. perniciosa* is highly expressed during the biotrophic interaction with cacao (Figure S4B), supporting the conclusion that *Moniliophthora* pathogens have evolved

inactive chitinases as an analogous strategy to chelate free chitin and prevent elicitation of the plant immune system. Because the mutated version of MpChi, in which we restored the enzymatic activity, is still able to prevent MTI (Figures S3C and S3D), we propose that loss of chitinolytic activity may have nonetheless conferred a selective advantage during evolution by turning this protein inert to the pathogen cell wall, reducing self-digestion and the resulting MAMP production. The fact that most *Moniliophthora* GH18 genes distinctively expressed *in planta* encode proteins with substitutions in key catalytic residues (Figure 3A) is in agreement with the idea that loss of enzymatic activity is an adaptation to the biological role of these proteins. Alternatively, the enzymatic activity of these proteins may not be detrimental to the pathogens during infection and was lost by genetic drift due to the absence of a strong selection pressure for its maintenance.

Effectors from filamentous pathogens are likely to arise from multiple independent evolutionary pathways, and many of them are enzymes that evolved to target plant components [32]. Notably, by showing that fungal pathogens can evolve effectors by repurposing the functions of enzymes that are conserved throughout evolution (i.e., neofunctionalization of chitinases), we shed light on an enigmatic and poorly documented topic: the birth of virulence factors. Given the recent observation that a family of effectors in parasitic nematodes evolved from the glutathione synthetase gene [33], that enzymatically inactive proteases in *Phytophthora* function as plant glucanase inhibitors [34, 35], and that *P. sojae* secretes a truncated inactive xyloglucanase as a decoy to protect its enzymatically active paralog from a host inhibitor [36], neofunctionalization of enzymes may constitute a widespread strategy for the evolution of virulence factors in pathogens as a whole. Genome mining revealed multiple instances of likely inactive GH18 chitinases in phytopathogenic fungi (Table S4), including *Blumeria graminis*, *Ceratocystis spp.*, *Colletotrichum spp.*, *Fusarium poae*, *Puccinia spp.*, *Rhizoctonia solani*, and *Valsa mali*. We anticipate that the scaffolds of chitinases and of other enzymes were likely co-opted to serve unexpected and yet-to-be-described virulence functions in pathogens.

STAR★METHODS

Detailed methods are provided in the online version of this paper and include the following:

SUPPLEMENTAL INFORMATION

Supplemental Information includes four figures and four tables and can be found with this article online at https://doi.org/10.1016/j.cub.2018.07.055.

ACKNOWLEDGMENTS

We thank Dr. Marc Nishimura and Dr. Jeff Dangl for comments on the draft of the manuscript; Dr. Victor Vitorello for sharing *Nicotiana tabacum* cells; and Dr. Andre Ambrosio, Dr. Sandra Dias, and Dr. Juliana Oliveira for advice and support on protein purification and with the use of the plate reader. We acknowledge the Protein Purification Facility (LPP) and the Spectroscopy and Calorimetry Facility (LEC) at the Brazilian Biosciences National Laboratory (LNBio), Centro Nacional de Pesquisa em Energia e Materiais (CNPEM), Campinas, for their support with the use of the fast protein liquid chromatography (FPLC) system and spectropolarimeter, respectively. We also thank the Central Laboratory of High-Performance Technologies (LaCTAD) at the State University of Campinas, Brazil, for their support with the use of the calorimeter. This research was supported by the São Paulo Research Foundation (FAPESP) through fellowships to G.L.F. (11/23315-1, 13/09878-9, and 14/06181-0) and P.J.P.L.T. (09/51018-1) and grants to G.A.G.P. (09/50119-9 and 16/10498-4).

AUTHOR CONTRIBUTIONS

Conceptualization, G.L.F. and P.J.P.L.T.; Data Curation, L.C.d.N.; Formal Analysis, L.C.d.N. and P.J.P.L.T.; Investigation, G.L.F., A.S.-V., D.P.d.T.T., P.F.V.d.P., and P.J.P.L.T.; Writing—Original Draft, G.L.F. and P.J.P.L.T.; Writing—Review & Editing, G.L.F., D.P.d.T.T., A.V.d.O.F., B.P.H.J.T., G.A.G.P., and P.J.P.L.T.; Resources, A.V.d.O.F. and B.P.H.J.T.; Supervision, G.A.G.P. and P.J.P.L.T.; Funding Acquisition, G.A.G.P.

DECLARATION OF INTERESTS

The authors declare no competing interests.

Received: May 17, 2018
Revised: July 3, 2018
Accepted: July 19, 2018
Published: September 13, 2018

REFERENCES

1. Fisher, M.C., Henk, D.A., Briggs, C.J., Brownstein, J.S., Madoff, L.C., McCraw, S.L., and Gurr, S.J. (2012). Emerging fungal threats to animal, plant and ecosystem health. Nature *484*, 186–194.
2. Jones, J.D., and Dangl, J.L. (2006). The plant immune system. Nature *444*, 323–329.
3. Win, J., Chaparro-Garcia, A., Belhaj, K., Saunders, D.G., Yoshida, K., Dong, S., Schornack, S., Zipfel, C., Robatzek, S., Hogenhout, S.A., and Kamoun, S. (2012). Effector biology of plant-associated organisms: concepts and perspectives. Cold Spring Harb. Symp. Quant. Biol. *77*, 235–247.
4. Lo Presti, L., Lanver, D., Schweizer, G., Tanaka, S., Liang, L., Tollot, M., Zuccaro, A., Reissmann, S., and Kahmann, R. (2015). Fungal effectors and plant susceptibility. Annu. Rev. Plant Biol. *66*, 513–545.
5. Felix, G., Regenass, M., and Boller, T. (1993). Specific perception of subnanomolar concentrations of chitin fragments by tomato cells: induction of extracellular alkalinization, changes in protein phosphorylation, and establishment of a refractory state. Plant J. *4*, 307–316.

6. Shibuya, N., and Minami, E. (2001). Oligosaccharide signalling for defence responses in plant. Physiol. Mol. Plant Pathol. *59*, 223–233.
7. Kaku, H., Nishizawa, Y., Ishii-Minami, N., Akimoto-Tomiyama, C., Dohmae, N., Takio, K., Minami, E., and Shibuya, N. (2006). Plant cells recognize chitin fragments for defense signaling through a plasma membrane receptor. Proc. Natl. Acad. Sci. USA *103*, 11086–11091.
8. Miya, A., Albert, P., Shinya, T., Desaki, Y., Ichimura, K., Shirasu, K., Narusaka, Y., Kawakami, N., Kaku, H., and Shibuya, N. (2007). CERK1, a LysM receptor kinase, is essential for chitin elicitor signaling in Arabidopsis. Proc. Natl. Acad. Sci. USA *104*, 19613–19618.
9. Sánchez-Vallet, A., Mesters, J.R., and Thomma, B.P. (2015). The battle for chitin recognition in plant-microbe interactions. FEMS Microbiol. Rev. *39*, 171–183.
10. de Jonge, R., van Esse, H.P., Kombrink, A., Shinya, T., Desaki, Y., Bours, R., van der Krol, S., Shibuya, N., Joosten, M.H., and Thomma, B.P. (2010). Conserved fungal LysM effector Ecp6 prevents chitin-triggered immunity in plants. Science *329*, 953–955.
11. Marshall, R., Kombrink, A., Motteram, J., Loza-Reyes, E., Lucas, J., Hammond-Kosack, K.E., Thomma, B.P., and Rudd, J.J. (2011). Analysis of two in planta expressed LysM effector homologs from the fungus *Mycosphaerella graminicola* reveals novel functional properties and varying contributions to virulence on wheat. Plant Physiol. *156*, 756–769.
12. Mentlak, T.A., Kombrink, A., Shinya, T., Ryder, L.S., Otomo, I., Saitoh, H., Terauchi, R., Nishizawa, Y., Shibuya, N., Thomma, B.P., and Talbot, N.J. (2012). Effector-mediated suppression of chitin-triggered immunity by *magnaporthe oryzae* is necessary for rice blast disease. Plant Cell *24*, 322–335.
13. Takahara, H., Hacquard, S., Kombrink, A., Hughes, H.B., Halder, V., Robin, G.P., Hiruma, K., Neumann, U., Shinya, T., Kombrink, E., et al. (2016). *Colletotrichum higginsianum* extracellular LysM proteins play dual roles in appressorial function and suppression of chitin-triggered plant immunity. New Phytol. *211*, 1323–1337.
14. Kombrink, A., Rovenich, H., Shi-Kunne, X., Rojas-Padilla, E., van den Berg, G.C., Domazakis, E., de Jonge, R., Valkenburg, D.J., Sánchez-Vallet, A., Seidl, M.F., and Thomma, B.P. (2017). *Verticillium dahliae* LysM effectors differentially contribute to virulence on plant hosts. Mol. Plant Pathol. *18*, 596–608.
15. Ploetz, R. (2016). The impact of diseases on cacao production: a global overview. In Cacao Diseases, B. Bailey, and L. Meinhardt, eds. (Springer), pp. 33–59.
16. Evans, H.C. (2007). Cacao diseases-the trilogy revisited. Phytopathology *97*, 1640–1643.
17. Teixeira, P.J., Thomazella, D.P., Reis, O., do Prado, P.F., do Rio, M.C., Fiorin, G.L., José, J., Costa, G.G., Negri, V.A., Mondego, J.M., et al. (2014). High-resolution transcript profiling of the atypical biotrophic interaction between *Theobroma cacao* and the fungal pathogen *Moniliophthora perniciosa*. Plant Cell *26*, 4245–4269.
18. Teixeira, P.J., Thomazella, D.P., and Pereira, G.A. (2015). Time for chocolate: current understanding and new perspectives on cacao witches' broom disease research. PLoS Pathog. *11*, e1005130.
19. Adrangi, S., and Faramarzi, M.A. (2013). From bacteria to human: a journey into the world of chitinases. Biotechnol. Adv. *31*, 1786–1795.
20. Hamid, R., Khan, M.A., Ahmad, M., Ahmad, M.M., Abdin, M.Z., Musarrat, J., and Javed, S. (2013). Chitinases: an update. J. Pharm. Bioallied Sci. *5*, 21–29.
21. Synstad, B., Gåseidnes, S., Van Aalten, D.M., Vriend, G., Nielsen, J.E., and Eijsink, V.G. (2004). Mutational and computational analysis of the role of conserved residues in the active site of a family 18 chitinase. Eur. J. Biochem. *271*, 253–262.
22. Watanabe, T., Ariga, Y., Sato, U., Toratani, T., Hashimoto, M., Nikaidou, N., Kezuka, Y., Nonaka, T., and Sugiyama, J. (2003). Aromatic residues within the substrate-binding cleft of *Bacillus circulans* chitinase A1 are essential for hydrolysis of crystalline chitin. Biochem. J. *376*, 237–244.
23. Horn, S.J., Sikorski, P., Cederkvist, J.B., Vaaje-Kolstad, G., Sørlie, M., Synstad, B., Vriend, G., Vårum, K.M., and Eijsink, V.G. (2006). Costs and benefits of processivity in enzymatic degradation of recalcitrant polysaccharides. Proc. Natl. Acad. Sci. USA *103*, 18089–18094.
24. Zakariassen, H., Aam, B.B., Horn, S.J., Vårum, K.M., Sørlie, M., and Eijsink, V.G. (2009). Aromatic residues in the catalytic center of chitinase A from *Serratia marcescens* affect processivity, enzyme activity, and biomass converting efficiency. J. Biol. Chem. *284*, 10610–10617.
25. van Loon, L.C., Rep, M., and Pieterse, C.M. (2006). Significance of inducible defense-related proteins in infected plants. Annu. Rev. Phytopathol. *44*, 135–162.
26. van den Burg, H.A., Harrison, S.J., Joosten, M.H., Vervoort, J., and de Wit, P.J. (2006). Cladosporium fulvum Avr4 protects fungal cell walls against hydrolysis by plant chitinases accumulating during infection. Mol. Plant Microbe Interact. *19*, 1420–1430.
27. Wu, S., Shan, L., and He, P. (2014). Microbial signature-triggered plant defense responses and early signaling mechanisms. Plant Sci. *228*, 118–126.
28. Meinhardt, L.W., Costa, G.G., Thomazella, D.P., Teixeira, P.J., Carazzolle, M.F., Schuster, S.C., Carlson, J.E., Guiltinan, M.J., Mieczkowski, P., Farmer, A., et al. (2014). Genome and secretome analysis of the hemibiotrophic fungal pathogen, *Moniliophthora roreri*, which causes frosty pod rot disease of cacao: mechanisms of the biotrophic and necrotrophic phases. BMC Genomics *15*, 164.
29. Pereira, J.F., Araújo, E.F., Brommonschenkel, S.H., Queiroz, C.B., Costa, G.G., Carazzolle, M.F., Pereira, G.A., and Queiroz, M.V. (2015). MpSaci is a widespread gypsy-Ty3 retrotransposon highly represented by non-autonomous copies in the *Moniliophthora perniciosa* genome. Curr. Genet. *61*, 185–202.
30. Aime, M.C., and Phillips-Mora, W. (2005). The causal agents of witches' broom and frosty pod rot of cacao (chocolate, *Theobroma cacao*) form a new lineage of *Marasmiaceae*. Mycologia *97*, 1012–1022.
31. Kerekes, J.F., and Desjardin, D.E. (2009). A monograph of the genera *Crinipellis* and *Moniliophthora* from Southeast Asia including a molecular phylogeny of the nrITS region. Fungal Divers. *37*, 101–152.
32. Franceschetti, M., Maqbool, A., Jiménez-Dalmaroni, M.J., Pennington, H.G., Kamoun, S., and Banfield, M.J. (2017). Effectors of filamentous plant pathogens: commonalities amid diversity. Microbiol. Mol. Biol. Rev. *81*, e00066-16.
33. Lilley, C.J., Maqbool, A., Wu, D., Yusup, H.B., Jones, L.M., Birch, P.R.J., Banfield, M.J., Urwin, P.E., and Eves-van den Akker, S. (2018). Effector gene birth in plant parasitic nematodes: Neofunctionalization of a housekeeping glutathione synthetase gene. PLoS Genet. *14*, e1007310.
34. Rose, J.K., Ham, K.S., Darvill, A.G., and Albersheim, P. (2002). Molecular cloning and characterization of glucanase inhibitor proteins: coevolution of a counterdefense mechanism by plant pathogens. Plant Cell *14*, 1329–1345.
35. Damasceno, C.M., Bishop, J.G., Ripoll, D.R., Win, J., Kamoun, S., and Rose, J.K. (2008). Structure of the glucanase inhibitor protein (GIP) family from phytophthora species suggests coevolution with plant endo-beta-1,3-glucanases. Mol. Plant Microbe Interact. *21*, 820–830.
36. Ma, Z., Zhu, L., Song, T., Wang, Y., Zhang, Q., Xia, Y., Qiu, M., Lin, Y., Li, H., Kong, L., et al. (2017). A paralogous decoy protects *Phytophthora sojae* apoplastic effector PsXEG1 from a host inhibitor. Science *355*, 710–714.
37. Pettersen, E.F., Goddard, T.D., Huang, C.C., Couch, G.S., Greenblatt, D.M., Meng, E.C., and Ferrin, T.E. (2004). UCSF Chimera–a visualization system for exploratory research and analysis. J. Comput. Chem. *25*, 1605–1612.
38. Andrews, S. (2010). FastQC: a quality control tool for high throughput sequence data (Babraham Bioinformatics).
39. Bolger, A.M., Lohse, M., and Usadel, B. (2014). Trimmomatic: a flexible trimmer for Illumina sequence data. Bioinformatics *30*, 2114–2120.
40. Kim, D., Langmead, B., and Salzberg, S.L. (2015). HISAT: a fast spliced aligner with low memory requirements. Nat. Methods *12*, 357–360.

41. Liao, Y., Smyth, G.K., and Shi, W. (2014). featureCounts: an efficient general purpose program for assigning sequence reads to genomic features. Bioinformatics *30*, 923–930.
42. Robinson, M.D., McCarthy, D.J., and Smyth, G.K. (2010). edgeR: a Bioconductor package for differential expression analysis of digital gene expression data. Bioinformatics *26*, 139–140.
43. Emms, D.M., and Kelly, S. (2015). OrthoFinder: solving fundamental biases in whole genome comparisons dramatically improves orthogroup inference accuracy. Genome Biol. *16*, 157.
44. Edgar, R.C. (2004). MUSCLE: multiple sequence alignment with high accuracy and high throughput. Nucleic Acids Res. *32*, 1792–1797.
45. Darriba, D., Taboada, G.L., Doallo, R., and Posada, D. (2011). ProtTest 3: fast selection of best-fit models of protein evolution. Bioinformatics *27*, 1164–1165.
46. Ronquist, F., and Huelsenbeck, J.P. (2003). MrBayes 3: Bayesian phylogenetic inference under mixed models. Bioinformatics *19*, 1572–1574.
47. Kelley, L.A., Mezulis, S., Yates, C.M., Wass, M.N., and Sternberg, M.J. (2015). The Phyre2 web portal for protein modeling, prediction and analysis. Nat. Protoc. *10*, 845–858.
48. Grosdidier, A., Zoete, V., and Michielin, O. (2011). SwissDock, a protein-small molecule docking web service based on EADock DSS. Nucleic Acids Res. *39*, W270–W277.
49. Letunic, I., and Bork, P. (2018). 20 years of the SMART protein domain annotation resource. Nucleic Acids Res. *46* (D1), D493–D496.
50. Miller, M.A., Pfeiffer, W., and Schwartz, T. (2010). Creating the CIPRES Science Gateway for inference of large phylogenetic trees. In 2010 Gateway Computing Environments Workshop (GCE), New Orleans, LA, 2010 (IEEE), pp. 1–8.
51. Letunic, I., and Bork, P. (2016). Interactive tree of life (iTOL) v3: an online tool for the display and annotation of phylogenetic and other trees. Nucleic Acids Res. *44*, W242–W245.
52. van den Burg, H.A., de Wit, P.J., and Vervoort, J. (2001). Efficient 13C/15N double labeling of the avirulence protein AVR4 in a methanol-utilizing strain (Mut+) of *Pichia pastoris*. J. Biomol. NMR *20*, 251–261.
53. Wass, M.N., Kelley, L.A., and Sternberg, M.J. (2010). 3DLigandSite: predicting ligand-binding sites using similar structures. Nucleic Acids Res. *38*, W469–W473.
54. Papanikolau, Y., Prag, G., Tavlas, G., Vorgias, C.E., Oppenheim, A.B., and Petratos, K. (2001). High resolution structural analyses of mutant chitinase A complexes with substrates provide new insight into the mechanism of catalysis. Biochemistry *40*, 11338–11343.
55. Uchiyama, T., Katouno, F., Nikaidou, N., Nonaka, T., Sugiyama, J., and Watanabe, T. (2001). Roles of the exposed aromatic residues in crystalline chitin hydrolysis by chitinase A from *Serratia marcescens* 2170. J. Biol. Chem. *276*, 41343–41349.
56. Tjoelker, L.W., Gosting, L., Frey, S., Hunter, C.L., Trong, H.L., Steiner, B., Brammer, H., and Gray, P.W. (2000). Structural and functional definition of the human chitinase chitin-binding domain. J. Biol. Chem. *275*, 514–520.
57. Edwards, K.D., Fernandez-Pozo, N., Drake-Stowe, K., Humphry, M., Evans, A.D., Bombarely, A., Allen, F., Hurst, R., White, B., Kernodle, S.P., et al. (2017). A reference genome for *Nicotiana tabacum* enables map-based cloning of homeologous loci implicated in nitrogen utilization efficiency. BMC Genomics *18*, 448.
58. McCarthy, D.J., Chen, Y., and Smyth, G.K. (2012). Differential expression analysis of multifactor RNA-seq experiments with respect to biological variation. Nucleic Acids Res. *40*, 4288–4297.
59. Robinson, M.D., and Oshlack, A. (2010). A scaling normalization method for differential expression analysis of RNA-seq data. Genome Biol. *11*, R25.
60. Benjamini, Y., and Hochberg, Y. (1995). Controlling the false discovery rate: a practical and powerful approach to multiple testing. J. R. Stat. Soc. B *57*, 289–300.
61. Warnes, G., Bolker, B., Bonebakker, L., Gentleman, R., Huber, W., Liaw, A., Tumley, T., Mächler, M., Magnusson, A., and Möller, S. (2016). gplots: various R programming tools for plotting data. https://cran.r-project.org/web/packages/gplots/index.html.
62. Livak, K.J., and Schmittgen, T.D. (2001). Analysis of relative gene expression data using real-time quantitative PCR and the 2(-Delta Delta C(T)) method. Methods *25*, 402–408.
63. Le, S.Q., and Gascuel, O. (2008). An improved general amino acid replacement matrix. Mol. Biol. Evol. *25*, 1307–1320.

STAR★METHODS

KEY RESOURCES TABLE

REAGENT or RESOURCE	SOURCE	IDENTIFIER
Bacterial and Virus Strains		
Escherichia coli Origami 2	Novagen	Cat#71345-3
Escherichia coli Shuffle T7	New England Biolabs	Cat#C3026J
Biological Samples		
Tomato hydrolytic extract	Bart Thomma, Wageningen University	N/A
Chemicals, Peptides, and Recombinant Proteins		
Crab shell chitin	Sigma-Aldrich	Cat#C7170
Chitin beads	New England Biolabs	Cat#S6651L
Chitosan	Sigma-Aldrich	Cat#C3646
Xylan	Sigma-Aldrich	Cat#X4252
Cellulose	Sigma-Aldrich	Cat#C6288
Chitohexaose (NAG6)	Isosep AB	Cat#56/11-0050
Chitohexaose (NAG6)	Santa Cruz Biotechnology	Cat#SC-222018
flg22	GenScript	Cat#RP19986
Critical Commercial Assays		
Chitinase Assay Kit	Sigma-Aldrich	Cat#CS1030
SuperScript II Reverse Transcriptase	Thermo Scientific	Cat#18064014
Sybr Green PCR Master Mix	Thermo Scientific	Cat#4309155
Deposited Data		
Raw RNA-seq reads and count matrix (*N. tabacum* BY-2 cells)	This paper	GEO: GSE111980
Raw RNA-seq reads (*M. roreri* x cacao interaction)	[28]	BioProject: PRJNA229176
MpChi nucleotide and protein sequences	This paper	GenBank: MH481742
MrChi nucleotide and protein sequences	This paper	GenBank: MH481743
Raw and analyzed data	This paper	Mendeley Data: https://doi.org/10.17632/dvdpg66fsj.1
Experimental Models: Cell Lines		
Nicotiana tabacum BY-2 cells	Victor Vitorello, University of São Paulo	N/A
Experimental Models: Organisms/Strains		
Moniliophthora perniciosa	Gonçalo Pereira, State University of Campinas	N/A
Theobroma cacao	Gonçalo Pereira, State University of Campinas	N/A
Trichoderma viride	Bart Thomma, Wageningen University	N/A
Oligonucleotides		
See Table S2 for the primers used for cloning, site-directed mutagenesis and qPCR assays	This paper	N/A
Recombinant DNA		
pET-6xHis-SUMO-MpChi	This paper	N/A
pET-6xHis-SUMO-MpChi^{Q167E}	This paper	N/A
pET-6xHis-SUMO-MpChi^{L238M}	This paper	N/A
pET-6xHis-SUMO-MpChi$^{Q167E/L238M}$	This paper	N/A
pET-6xHis-SUMO-MpChi^{MBS}	This paper	N/A
pET-6xHis-SUMO-MrChi	This paper	N/A
pET-6xHis-SUMO-MrChi^{N135D}	This paper	N/A

(*Continued on next page*)

Continued

REAGENT or RESOURCE	SOURCE	IDENTIFIER
pET-6xHis-SUMO-MR05413	This paper	N/A
pET-6xHis-SUMO-Ecp6	This paper	N/A
Software and Algorithms		
UCSF Chimera v1.12	[37]	RRID:SCR_004097
FastQC v.0.11.5	[38]	RRID:SCR_014583
Trimmomatic v0.36	[39]	RRID:SCR_011848
HiSat2 v2.0.5	[40]	RRID:SCR_015530
featureCounts v1.5.2	[41]	RRID:SCR_012919
edgeR v3.16.1	[42]	RRID:SCR_012802
Orthofinder	[43]	https://github.com/davidemms/OrthoFinder
MUSCLE v3.8	[44]	RRID:SCR_011812
prottest v3.4.2	[45]	RRID:SCR_014628
MrBayes v3.2.6	[46]	RRID:SCR_012067
Origin	OriginLab	RRID:SCR_014212
R v3.4	The R Project for Statistical Computing	RRID:SCR_001905
RStudio v1.1	https://www.rstudio.com/	RRID:SCR_000432
Other		
WBD Transcriptome Atlas	[17]	http://www.lge.ibi.unicamp/br/wbdatlas
Phyre2	[47]	http://www.sbg.bio.ic.ac.uk/~phyre2/
SwissDock	[48]	http://www.swissdock.ch/
SMART	[49]	http://smart.embl-heidelberg.de/
CIPRES Portal	[50]	https://www.phylo.org/
iTOL	[51]	https://itol.embl.de/

CONTACT FOR REAGENT AND RESOURCE SHARING

Further information and requests for resources and reagents should be directed to and will be fulfilled by the Lead Contact, Paulo José Pereira Lima Teixeira (paulojt@email.unc.edu).

EXPERIMENTAL MODEL AND SUBJECT DETAILS

The *MpChi* gene was cloned using a cDNA sample prepared from plants infected with the *Moniliophthora perniciosa* isolate BP10. Cacao plants (cultivar 'Comum') used in the gene expression experiments were either grown in a greenhouse (infected shoots) [17] or in a farm located in Ilhéus, Brazil (infected fruits). *Nicotiana tabacum* BY-2 cells were used in the pH shift experiments. Cells were maintained in liquid Murashige and Skoog medium (supplemented with 30 g/L sucrose, 1 mg/L 2,4-Dichlorophenoxyacetic acid, 0.1 mg/L kinetin and 1X Gamborg's vitamins) in the dark at 27°C and 100 rpm and were subcultured weekly. The *Trichoderma viride* strain B197 was used in the fungal cell wall protection assays.

METHOD DETAILS

Production of recombinant proteins

The coding sequence of the *MpChi* gene (minus the region encoding the signal peptide) was amplified by PCR using cDNA made from an infected cacao plant as the template and sub-cloned into pGEM-T Easy (Promega). The modified versions $MpChi^{Q167E}$, $MpChi^{L238M}$ and $MpChi^{Q167E/L238M}$ were obtained from the pGEM-MpChi clone using the QuickChange Site-Directed Mutagenesis Kit (Stratagene) following the manufacturer's protocol. $MpChi^{MBS}$, *MrChi* and *MR05413* were synthesized (GenScript and Eurofins) without the signal peptide sequence with codons optimized for *Escherichia coli*. The sequences of all primers used in this study are provided in Table S2.

For protein expression, the cloned DNA fragments were transferred to a modified version of pET SUMO (Invitrogen), confirmed by Sanger sequencing and transformed into *E. coli* Origami 2 (Novagen) or Shuffle T7 (New England Biolabs). Bacterial cells were grown

at 37°C until the culture achieved an optical density of approximately 0.8. Then, IPTG was added to induce protein expression and cells were grown overnight at 18°C. Table S3 presents the conditions used for the expression of each protein.

Cells were harvested by centrifugation and suspended in lysis buffer (50 mM Tris-HCl pH 8.5, 300 mM NaCl, 10% glycerol, 6 mg/mL lysozyme, 2 mg/mL sodium deoxycholate, 20 μg/mL DNase, 1 mM PMSF). After lysis for 1 hour at 0°C, the culture was centrifuged to remove cellular debris and the cleared supernatant was used for protein purification. His_6-SUMO-tagged proteins were purified by immobilized metal ion affinity chromatography (IMAC) using a Co^{2+}-charged TALON Resin (Clontech Laboratories) pre-equilibrated with 50 mM Tris-HCl pH 8,5 and 300 mM NaCl. After elution from the resin, the protease ULP-1 was used to remove the His_6-SUMO tag and a second round of IMAC was performed to allow the separation of the recombinant protein from the tag. Protein concentration was determined spectrophotometrically at 280 nm. Clones and expression methods for *Avr4* and *Ecp6* were described previously [10, 52].

Circular dichroism

Circular dichroism (CD) spectra were recorded on a J810 spectropolarimeter (Jasco) at 20°C from 195 nm to 260 nm with a resolution of 0.5 nm. The molar concentrations used to calculate the molar ellipticity (θ) were the following: MpChi: 2.5 μM; $MpChi^{Q167E}$: 3 μM; $MpChi^{L238M}$: 2.5 μM; $MpChi^{Q167E/L238M}$: 2.5 μM; $MpChi^{MBS}$: 3 μM; MrChi: 2.5 μM; $MrChi^{N135D}$: 3.7 μM; MR05413: 5 μM. Each data point was generated by averaging 10 accumulations.

Structural modeling

Homology modeling of MpChi (residues 24-438; signal peptide removed) was performed with the Phyre2 suite using the normal modeling mode [47]. The final model presented a confidence score of 100% and a coverage of 94% and was based on a GH18 chitinase from *Chromobacterium violaceum* (Protein Data Bank ID 4TXG; 100% confidence and 22% identity). Prediction of binding sites was performed with 3DLigandSite [53] and matched previous experimental evidence for GH18 proteins [21, 22, 24, 54, 55]. Molecular docking was performed on the SwissDock server [48] using NAG6 as the ligand. Visualization and edition of the model was done with UCSF Chimera v1.12 [37].

Polysaccharide pull-down assay

Carbohydrate affinity precipitation assays were performed as described by Tjoelker et al. (2000) [56]. Binding to crab shell chitin (Sigma-Aldrich), chitin beads (New England Biolabs), chitosan (Sigma-Aldrich), xylan (Sigma-Aldrich) and cellulose (Sigma-Aldrich) was tested by incubating 50 μg of recombinant protein with 10 mg of each insoluble carbohydrate in 800 μL of water. After three hours of rocking (200 rpm) at room temperature, the insoluble (carbohydrate-bound) fraction was precipitated by centrifugation at 14,000 × g for 5 minutes and the supernatant was reserved. The insoluble fraction was washed five times with PBS buffer (137 mM NaCl, 2.7 mM KCl, 10 mM Na_2HPO_4, 2 mM KH_2PO_4, pH 7.2) and then boiled in the presence of 1% SDS to dissociate the proteins from the substrate. Presence of the proteins in the supernatant and in the precipitate was verified by SDS-PAGE and Coomassie Brilliant Blue staining.

Isothermal titration calorimetry

Isothermal titration calorimetry (ITC) was performed to determine the affinity of MpChi to chitin oligosaccharides of six units (NAG6; Isosep AB, Tullinge, Sweeden). Recombinant MpChi at a concentration of 20 μM was titrated with a 2 μL injection followed by 15 injections of 8 μL NAG6 at 200 μM. Chitin oligomers and the protein were suspended in PBS (137 mM NaCl, 2.7 mM KCl, 10 mM Na_2HPO_4, 2 mM KH_2PO_4, pH 7.2). Measurements were performed at 25°C using the Microcal VP-ITC calorimeter (GE-Healthcare). A second round of ITC experiments was performed for MpChi, $MpChi^{MBS}$ and MrChi in parallel using the MicroCal iTC200 calorimeter (GE-Healthcare). For this, each protein at a concentration of 15 μM in the sample cell was titrated with a 0.5 μL injection followed by 19 injections of 2 μL NAG6 (Santa Cruz Biotechnology) at 150 μM. Like in the first experiment, proteins and NAG6 were suspended in PBS and measurements were carried out at 25°C. Data was analyzed with the program Origin (OriginLab) and fitted to the model describing one binding site.

Chitinolytic activity assay

Chitinolytic activity was measured using the fluorimetric Chitinase Assay Kit (Sigma-Aldrich) following the manufacturer's instructions. Three different substrates were used to allow the detection of different types of chitinolytic activities: 4-Methylumbelliferyl-N,N-diacetyl-β-D-chitobioside (exochitinase activity - chitobiosidase), 4-Methylumbelliferyl-N-acetyl-β-D-glucosaminide (exochitinase activity- N-acetylglucosaminidase) and 4-Methylumbelliferyl-β-D-N,N′,N″-triacetylchitotrioside (endochitinase activity). Cleavage of these substrates releases 4-methylumbelliferone (4MU), which can be measured fluorimetrically at an excitation wavelength of 360 nm and an emission wavelength of 450 nm. Measurements were done by incubating 100 ng of recombinant protein with each of the three substrates for 30 minutes at 37°C. Fluorescence was detected with an EnSpire Multimode Reader (PerkinElmer). Each measurement was performed in triplicate and experiments were repeated at least four times with independent batches of recombinant proteins.

Fungal cell wall protection assay

To test whether MpChi is able to protect fungal hyphae against plant hydrolytic enzymes, we performed the spore protection assay described previously [10, 26]. A 40 μL aliquot of *Trichoderma viride* spores at a concentration of 50,000 conidia/mL was incubated overnight in PDB (Potato Dextrose Agar, Difco) at 22°C in a 96-well plate. Subsequently, 10 μL of recombinant proteins (Avr4, Ecp6 or MpChi) at 100 μM were added individually to the spores (final concentration of 20 μM). After 2 h of incubation at room temperature, 10 μL of a tomato hydrolytic extract were added and the plate was incubated at room temperature for 24 h. Fungal growth was then visualized microscopically. The experiment was repeated three times and each repetition contained three biological replicates.

Medium alkalinization experiments

Medium alkalinization of plant cell cultures was used as a proxy for MTI initiation upon treatment with MAMPs. *Nicotiana tabacum* BY-2 cell suspensions (3 – 5 days-old) were transferred to 12-well plates (2.5 mL/well) and kept at room temperature with gentle rocking for at least 2 h. Cells were treated with 10 nM NAG6 (Santa Cruz Biotechnology), 100 nM flg22 (GenScript) or 100 nM of recombinant proteins. Mixtures of elicitors and proteins were kept at room temperature for at least 10 minutes before addition to plant cells. Following the treatment, the pH of the cell suspension was measured over 10 minutes in intervals of 3 s using a S220-Basic Seven Compact pHmeter equipped with an InLab Micro electrode (Mettler Toledo). The Ecp6 effector protein from *C. fulvum* was used as a positive control. In experiments that used flg22 as the elicitor molecule, the pH was monitored for 60 minutes.

Gene expression analyses by RNA-seq

MpChi was initially identified as one of the most highly expressed fungal genes during the biotrophic interaction between *M. perniciosa* and cacao [17]. Transcript levels in multiple stages of the pathogen life cycle and during the progression of witches' broom disease was evaluated using the WBD Transcriptome Atlas (http://www.lge.ibi.unicamp.br/wbdatlas). This database is a collection of RNA-seq libraries constructed from multiple biological conditions and includes a wide range of developmental stages, growth conditions and stress responses of the fungus – either *in vitro* and *in planta*. Normalized expression values are given in RPKM (reads per kilobase of transcript per million mapped reads) and are available at the Mendeley Data repository (https://doi.org/10.17632/dvdpg66fsj.1). Details of data analysis are described by Teixeira et al. 2014 [17]. For the analysis of *M. roreri* gene expression, RNA-seq reads derived from the biotrophic (30 days after infection) and necrotrophic (60 days after infection) stages of frosty pod rot [28] were aligned against the 17,920 gene models of the pathogen using bowtie, then counted and normalized to RPKM values for plotting.

To evaluate the ability of MpChi in preventing the transcriptional response downstream of MAMP perception, *Nicotiana tabacum* BY-2 cells were treated with 10 nM NAG6, 100 nM MpChi, 10 nM NAG6 + 100 nM MpChi or H_2O (Mock treatment) as described above (Medium alkalinization experiments). Samples were harvested immediately before the start of the experiment (Time 0, untreated cells) and at four time points after the treatment (15 min, 60 min, 120 min and 180 min). The experiment was performed in triplicate. RNA was extracted using the TRIzol Reagent (Invitrogen) following the manufacturer's protocol and then used to prepare RNA-seq libraries. The resulting 54 libraries were pooled and sequenced in one lane of a HiSeq2500 instrument to generate 50bp single-end reads. Initial assessment of raw sequences was done with FastQC v.0.11.5 [38]. Trimmomatic v0.36 [39] was used to remove adaptor-containing and low-quality reads. Quality-filtered reads were then aligned against the 69,500 cDNA sequences of the *Nicotiana tabacum* K236 v4.5 reference [57] using HiSat2 v2.0.5 [40] and counted with featureCounts v1.5.2 [41]. Identification of differentially expressed genes was done using the generalized linear model (glm) approach [58] implemented in the edgeR package v3.16.1 [42]. To filter out weakly expressed genes, only those genes with a minimum expression level of 1 count per million in at least 3 libraries were included in the analysis. Normalization was performed using the trimmed mean of M-values method (TMM) [59]. A one-way-layout model was used to compare the treatments (NAG6, MpChi or MpChi+NAG6) to the control condition (H_2O) at each of the four time-points. The Benjamini–Hochberg method (false discovery rate; FDR) was used for the correction of multiple comparisons [60]. Genes with FDR below or equal to 0.01 and a fold-change variation of at least 1.5x were considered differentially expressed. The full edgeR results are provided in the Mendeley Data repository (https://doi.org/10.17632/dvdpg66fsj.1). Raw RNA-seq reads and the count matrix generated in this study are available at the NCBI Gene Expression Omnibus under the accession number GEO: GSE111980.

Hierarchical clustering was performed in R with the 'heatmap.2' function from the gplots package [61]. RPKM expression values of genes identified as differentially expressed in at least one of the treatments in the experiment were normalized by z-score transformation. Genes were clustered on the basis of the Euclidean distance and with the complete-linkage method.

Gene expression analyses by qPCR

As a complementation to the RNA-seq data available at the WBD Transcriptome Atlas (http://www.lge.ibi.unicamp.br/wbdatlas), transcript levels of the *MpChi* gene were determined by qPCR in a subset of nine biological conditions: monokaryotic mycelium, dikaryotic mycelium, basidiomata, spores, germinating spores and infected shoots and fruits at the biotrophic and necrotrophic stages of the infection. This experiment included three biological replicates per condition. qPCRs were conducted on a ViiA 7 Real-Time PCR System (Applied Biosystems) using SYBR Green I for the detection of PCR products. Each reaction was performed in technical triplicates and had a final volume of 12 μL, containing 6 μL SYBR Green PCR Master Mix (Thermo Scientific), 200 nM each primer, and 40 ng cDNA template. The thermal cycling conditions were 95°C for 10 min, followed by 40 cycles of 95°C for 15 s and 60°C for 1 min, with fluorescence detection at the end of each cycle. A melting curve analysis was conducted to confirm the amplification of a single

product per reaction. The *MpChi* mRNA relative abundance was defined by the mathematical model described by Livak and Schmittgen (2001) [62] using the *M. perniciosa* β-*actin* and *IF3b* (transcription initiation factor) genes as normalizers. Primers used in these experiments are given in Table S2.

Phylogenetic analyses

Genes encoding GH18 proteins were identified in *M. perniciosa* (CP02) and *M. roreri* (MCA2977) through a combination of manual Blast searches and orthogroups inference [43]. The GH18 domains were then annotated using SMART [49] and aligned with MUSCLE v3.8 [44]. The alignment was curated by removing sites containing gaps. Prior to the construction of the phylogenetic tree, prottest v3.4.2 [45] was used to determine the best-fit substitution model for the data. A Bayesian phylogenetic analysis was then performed with MrBayes v3.2.6 [46] on the CIPRES Portal [50] using the LG + G substitution model [63]. The MCMC analysis used 4 chains (1 cold), 1 million generations sampled every 100 generations and a burn-in value of 2500 (25%). The resulting tree was loaded into iTOL [51] and annotated with RNA-seq gene expression values (in RPKM) derived from cacao fruits infected with *M. perniciosa* or *M. roreri* at the biotrophic and necrotrophic stages of the infection.

Search for likely inactive GH18 chitinases in fungi

We searched for additional examples of GH18 proteins with substitutions in important catalytic residues in other fungal species (Table S4). To this end, we performed a PHI-BLAST search in the NCBI nr database (filtered for fungi - Taxid 4751) using the MpChi amino acid sequence and a modified version of the PROSITE pattern of the active site of GH18 chitinases: [LIVMFY]-[DN]-G-[LIVMF]-x-[LIVMF]-x-x-[ARNDCQGHILKMFPSTWYV]. This modified pattern restricts the output to proteins that do not have the critical glutamate (E) in the motif DxDxE, while allowing any amino acid in the positions of the conserved aspartates (D). By filtering hits that do not have the conserved glutamate, we focus on proteins that are very unlikely to have enzymatic activity.

QUANTIFICATION AND STATISTICAL ANALYSIS

All statistical analyses described in this study were performed using R. Number of replicates for each experiment is reported in the figure legends. For the qPCR and chitinase activity assays, statistical comparison among groups was performed by one-way ANOVA with the Tukey's Honest Significant Difference (HSD) post hoc test. Identification of differentially expressed genes in RNA-seq was performed with the generalized linear model (glm) approach implemented in the edgeR package.

DATA AND SOFTWARE AVAILABILITY

Source data of the results presented in this work, including uncropped gels, protein model (PDB format), amino acid alignments, original pH shift and enzymatic activity measurements, ITC files and the results of the identification of differentially expressed genes using edgeR were deposited in the Mendeley Data repository (https://doi.org/10.17632/dvdpg66fsj.1). Raw sequences and the read count matrix from the RNA-seq experiment are available at the NCBI Gene Expression Omnibus under the accession number GEO: GSE111980. A gene expression database constructed from a range of life stages and growth conditions of *M. perniciosa* is available at the WBD Transcriptome Atlas (http://www.lge.ibi.unicamp/br/wbdatlas). The accession numbers for the nucleotide and protein sequences of MpChi and MrChi reported in this paper are GenBank: MH481742, and MH481743.

Current Biology, Volume *28*

Supplemental Information

Suppression of Plant Immunity by Fungal Chitinase-like Effectors

Gabriel Lorencini Fiorin, Andrea Sanchéz-Vallet, Daniela Paula de Toledo Thomazella, Paula Favoretti Vital do Prado, Leandro Costa do Nascimento, Antonio Vargas de Oliveira Figueira, Bart P.H.J. Thomma, Gonçalo Amarante Guimarães Pereira, and Paulo José Pereira Lima Teixeira

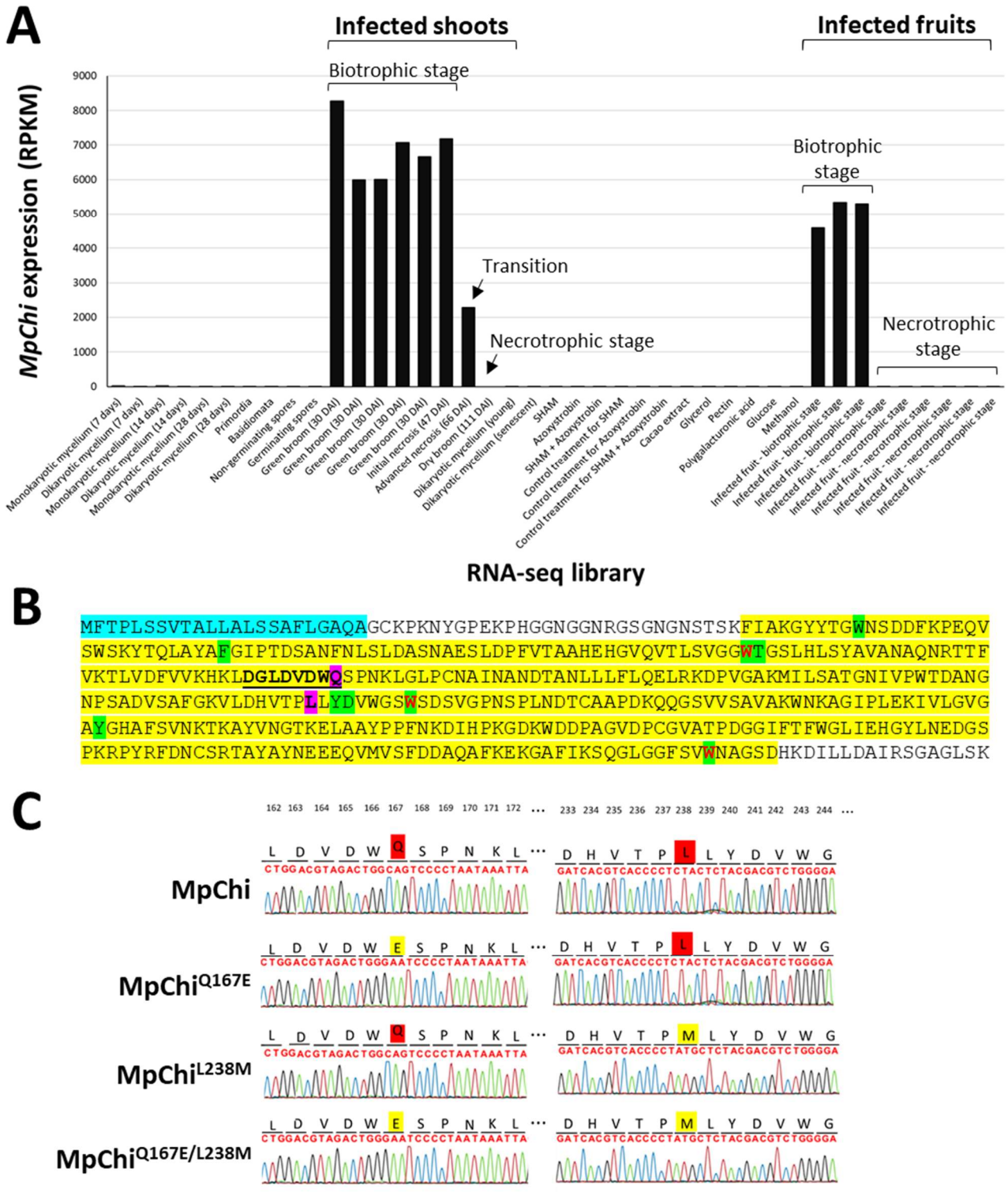

Figure S1. MpChi is highly expressed during the biotrophic stage of witches' broom disease and encodes a GH18 protein with substitutions in catalytic residues, Related to Figure 1 and Figure 2.

(A) Data is derived from the Witches' broom disease RNA-seq Atlas (www.lge.ibi.unicamp.br/wbdatlas) and includes 41 RNA-seq libraries from different biological conditions of the fungus either *in vitro* and *in planta*. Stages representing the disease progression in shoots and in fruits are labeled. Gene expression levels are

presented as RPKM (Reads Per Kilobase of transcript per Million mapped reads). Raw values of each library are provided in the Mendeley Data repository (doi:10.17632/dvdpg66fsj.1).

(B) MpChi is 438 amino acids long, with the first 23 residues corresponding to the predicted signal peptide for secretion (highlighted in light blue). The GH18 domain is highlighted in yellow. The catalytic motifs of GH18 chitinases is underlined (typical consensus DXXDXDXE). The two substituted residues identified in MpChi (Q167 and L238) are shown in purple. Substrate-binding residues predicted by 3DLigandSite are shown in green and overlap with amino acids experimentally validated in previous studies with GH18 chitinases. The three tryptophans denoted in red font were replaced by alanines in MpChi^{MBS} (see Figure 2).

(C) Artificial reversion of the catalytic residues in MpChi by site directed mutagenesis. Amino acid sequences are shown along with the DNA sequence (Sanger sequencing chromatogram). Residues in red were modified in one or more mutants (yellow).

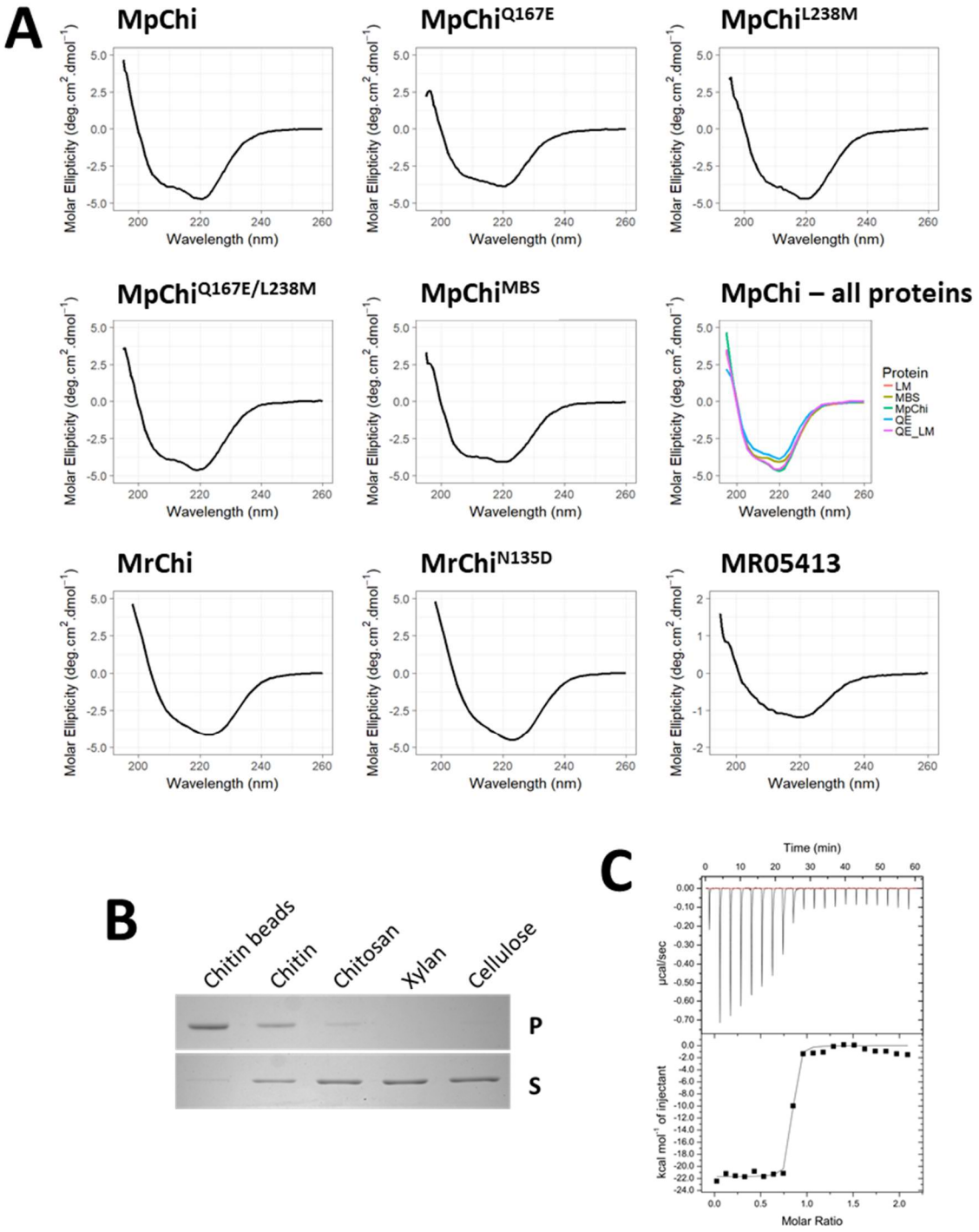

Figure S2. Controls for recombinant proteins used in this study, Related to Figure 1, Figure 2 and Figure 3.

(A) Circular dichroism spectra indicate that all proteins are properly folded and thus the artificial mutations introduced in MpChi and MrChi did not lead to drastic conformational changes.

(B) Pull-down assay demonstrates that MrChi binds to chitin but not to chitosan, xylan or cellulose.

(C) Isothermal titration calorimetry (ITC) shows that MrChi binds to chitin oligomer (NAG6) with high affinity (Kd = 10 nM).

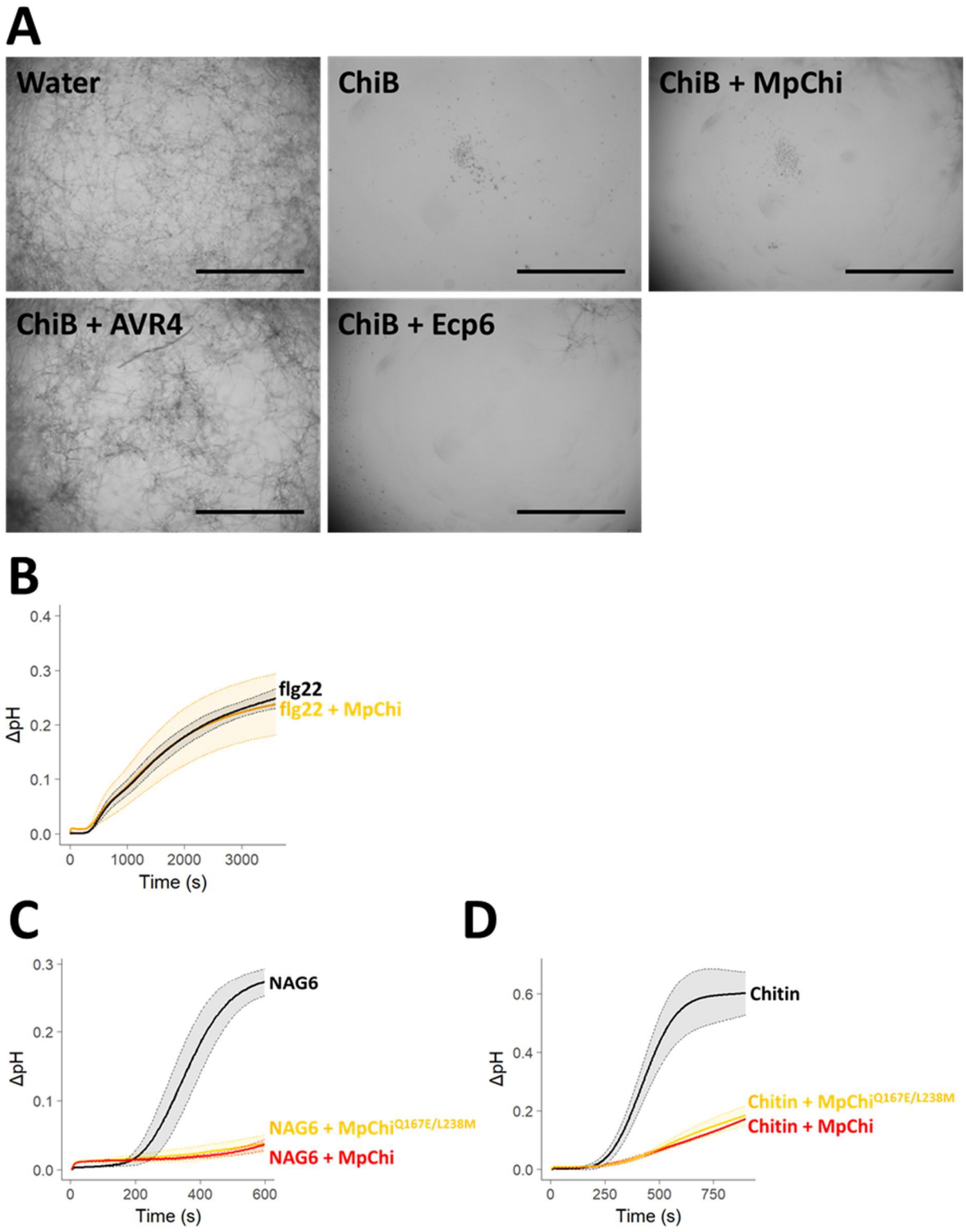

Figure S3. MpChi does not protect fungal hyphae against plant hydrolytic enzymes nor prevents flg22-triggered medium alkalinization. Despite being enzymatically active, MpChi$^{Q167E/L238M}$ retains the ability to prevent MTI following chitin or chitin oligomers treatment, Related to Figure 2.

(A) Spores of *Trichoderma viride* were treated with water, crude extract of tomato leaves containing intracellular basic chitinases (ChiB), pretreatment with 100 µM MpChi followed by addition of tomato hydrolytic extract (ChiB + MpChi), pretreatment with 100 µM Avr4 followed by addition of tomato hydrolytic extract (ChiB + Avr4; positive

control) and pretreatment with 100 µM Ecp6 followed by addition of tomato hydrolytic extract (ChiB + Ecp6; negative control). Micrographs were taken 24h after treatment. The experiment was repeated three times and each repetition contained three biological replicates.

(B) Medium alkalinization induced by the treatment of tobacco cells with 100 nM flg22 cannot be prevented by MpChi. The graphic shows the pH shift of the medium over 60 min after treatment with the elicitor.

(C) Medium alkalinization induced by the treatment of tobacco cells with 10 nM chitin oligomers (NAG6) is prevented by both MpChi and MpChi$^{Q167E/L238M}$. The graphic shows the pH shift of the medium over 10 min after treatment with the elicitor.

(D) Medium alkalinization induced by the treatment of tobacco cells with 100 µg/mL chitin is prevented by both MpChi and MpChi$^{Q167E/L238M}$. The graphic shows the pH shift of the medium over 15 min after treatment with the elicitor.

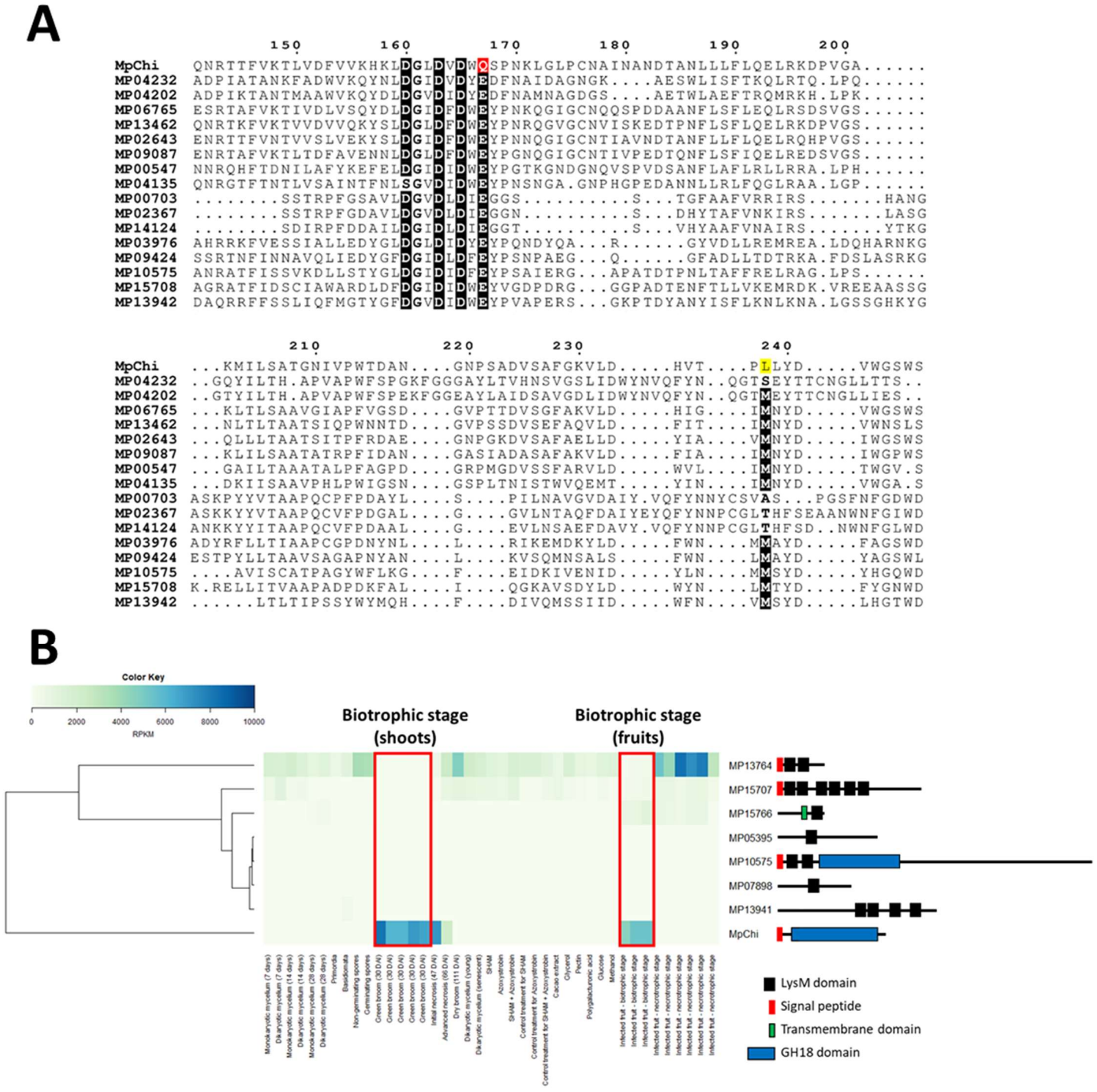

Figure S4. The *M. perniciosa* genome (CP02) encodes 17 GH18 and 7 LysM proteins, Related to Figure 3 and Figure 4.

(A) Alignment of *M. perniciosa* GH18 proteins. A total of 17 genes encoding proteins belonging to the GH18 family were identified in the *M. perniciosa* genome (isolate CP02). The region containing the canonical catalytic motif of GH18 chitinases (DxxDxDxE) and the conserved methionine are shown. MpChi is the only protein presenting substitutions in both the glutamate (Q167; red) and the methionine (L238; yellow) of the catalytic site. Numbers on the top refer to the MpChi sequence.

(B) Expression profile of LysM-encoding genes found in the *M. perniciosa* genome (CP02). The heatmap shows the expression values (in RPKM) of the seven *M. perniciosa* LysM genes and of *MpChi* in 41 different RNA-seq libraries. *MpChi* is the only gene that is distinctively expressed during the fungal biotrophic interaction with cacao.

A scheme representing the domain organization of each gene is shown on the right. Only three of the seven LysM-containing proteins have a signal peptide for secretion. These results suggest that LysM effectors do not play a significant role on the *M. perniciosa* virulence on cacao.

Table S1. Most highly expressed *M. perniciosa* genes during the biotrophic interaction with cacao (green broom stages), Related to Figure 1 and Figure S1. *MpChi* is highlighted in yellow. The *M. perniciosa* genome has a total of 17.008 predicted genes. Gene expression values in RPKM are the average of five biological replicates.

Rank	GeneID	Gene description	Secreted?	RPKM
1	MP13831	No hits	X	78989.69
2	MP14755	No hits	X	68876.07
3	MP14757	No hits	X	26386.15
4	MP15869	No hits		21578.01
5	MP13352	MpPR-1g	X	16929.75
6	MP15868	Hypothetical protein	X	11597.29
7	MP16558	No hits	X	10963.53
8	MP09913	No hits	X	9990.17
9	MP14724	No hits		9553.71
10	MP13834	No hits	X	9246.93
11	MP13136	No hits	X	8508.95
12	MP09729	Alcohol dehydrogenase		8239.51
13	MP09537	glycoside hydrolase family 18 protein	X	6805.40
14	MP15315	MpCP12 (Cerato-platanin)	X	5339.45
15	MP15025	endoglucanase v-like protein	X	4762.20
16	MP15342	endo-polygalacturonase		4339.83
17	MP16511	MpCP11 (Cerato-platanin)	X	4049.07
18	MP04874	translation elongation factor ef1-alpha		4024.85
19	MP12125	MpPR-1h	X	4024.30
20	MP15312	MpCP4 (Cerato-platanin)	X	3860.01
21	MP10165	No hits	X	3821.21
22	MP09883	polyubiquitin		3712.83
23	MP13564	glycoside hydrolase family 5 protein	X	3603.68
24	MP02535	No hits	X	3452.10
25	MP14822	No hits		3424.51
26	MP12830	MpCP5 (Cerato-platanin)	X	3354.27
27	MP11627	1 concanamycin induced protein c		2904.36
28	MP09490	manganese superoxide dismutase		2866.45
29	MP16537	No hits	X	2802.44
30	MP14639	hypothetical protein		2769.59
31	MP06453	MpPR-1f	X	2344.58
32	MP07714	No hits	X	2239.28
33	MP12097	peptidyl-prolyl cis-trans isomerase		2172.16
34	MP04948	beta-ig-h3 fasciclin	X	2158.28
35	MP12214	CBD9-like protein		2015.46

Table S2. Primers used in this study, Related to STAR Methods.

Gene	Description	Forward Primer (5'→3')	Reverse Primer (5'→3')
MpChi	Gene amplification from green broom cDNA with addition of flanking restriction sites (EcoRI and HindIII)	GAATTCGGATGCAAACCGAAAAATTACG	AAGCTTCTACTTGGACAATCCGGCAC
$MpChi^{Q167E}$	Q167→E substitution in MpChi (targeted codon underlined)	CTGGACGTAGACTGGGAATCCCCTAATAAATTA	TAATTTATTAGGGGATTCCCAGTCTACGTCCAG
$MpChi^{L238M}$	L238→M substitution in MpChi (targeted codon underlined)	GATCACGTCACCCCTATGCTCTACGACGTCTG	CAGACGTCGTAGAGCATAGGGGTGACGTGATC
$MrChi^{N135D}$	N135→D substitution in MrChi (targeted codon underlined)	GACTGCATCGACCTGGACTGGGAATACCCGGCG	CGCCGGGTATTCCCAGTCCAGGTCGATGCAGTC
MR05413	Gene amplification for cloning into pET-SUMO with addition of flanking restriction sites (SacI and NotI)	GAGCTCCGATGCGCACCGAAGAATTATC	GCGGCCGCCTACTTTGACAATCCAG
Ecp6	Gene amplification for cloning into pET-SUMO with addition of flanking restriction sites (BamHI and NotI)	GGATCCGAGACCAAGGCCACAGACTG	GCGGCCGCTTATGCCACAGCAGTAGTGACG
MpChi_qPCR	Quantification of MpChi transcripts by qPCR	TGGTCCAAGTATACGCAGTTG	AGCAGTAACAAAGGGATCAAGG
MpActin_qPCR	Quantification of MpAct transcripts by qPCR	CCCTTCTATCGTCGGTCGT	AGGATACCACGCTTGGATTG
MpIF3b_qPCR	Quantification of MpIF3b transcripts by qPCR	CCCTGTAGAAGTCGTGGAATTG	GACAATGGCAAATCGTTCTCC

Table S3. Summary of the conditions used to produce each recombinant protein in this study, Related to STAR Methods. All genes were clone into a modified version of the pET-SUMO vector, which adds a SUMO and a His_6 tag to the N-terminal end of the protein.

Protein	*E. coli* strain	Temperature (ºC)	IPTG (mM)	Induction time
MpChi	Origami 2	18	0.05	Overnight
$MpChi^{Q167E}$	Origami 2	18	0.05	Overnight
$MpChi^{L238M}$	Origami 2	18	0.05	Overnight
$MpChi^{Q167E/L238M}$	Origami 2	18	0.05	Overnight
$MpChi^{MBS}$	Origami 2	18	0.05	Overnight
MR04303	Shuffle T7	18	0.2	Overnight
MR05413	Shuffle T7	18	0.05	Overnight
Ecp6	Origami 2	18	0.2	Overnight